

## Synchrotron-radiation photoemission studies of interface formation between metals and superconductors: Al and In on $\text{YBa}_2\text{Cu}_3\text{O}_{6.9}$

Y. Gao, I. M. Vitomirov, C. M. Aldao, T. J. Wagener, J. J. Joyce, C. Capasso, and J. H. Weaver  
*Department of Chemical Engineering and Materials Science, University of Minnesota, Minneapolis, Minnesota 55455*

D. W. Capone II

*Materials Science Division, Building 223, Argonne National Laboratory, Argonne, Illinois 60439*

(Received 16 October 1987)

The interfaces formed when the group-III $A$  metals Al and In are deposited onto the high-temperature superconductor  $\text{YBa}_2\text{Cu}_3\text{O}_{6.9}$  have been studied using high-resolution synchrotron-radiation photoelectron spectroscopy. Both Al and In deplete oxygen from the substrate to form their own oxides, which efficiently prevent further reaction between the substrate and the deposited metal. Subsequent deposition of metallic Al or In results in the formation of clusters. These heterogeneously reacted interfaces therefore exhibit superconducting, insulating, and metallic phases.

The recent discovery of high-temperature superconductors has stimulated intense activity because of their great promise for science and technology.<sup>1</sup> Photoelectron spectroscopy<sup>2-8</sup> (PES), inverse photoelectron spectroscopy<sup>9,10</sup> (IPES), and ground-state band-structure calculations have provided insight into the electronic states and serve as the starting point for understanding the mechanisms of the superconductivity.<sup>11-15</sup>

In this paper we report the first high-resolution synchrotron-radiation photoemission study of interface formation between metals and the high-temperature superconductor  $\text{YBa}_2\text{Cu}_3\text{O}_{6.9}$ . The group-III $A$  metals were chosen because of their importance in thin-film technologies (Al is the most frequently used metal for interconnects) and because Al forms a very stable oxide which could serve as an inexpensive protecting layer for high- $T_c$  materials, provided that it did not have a detrimental effect on the superconductor surface. Our results show that both Al and In react by withdrawing oxygen and forming oxides. At room temperature, this oxidation process is self-limiting since the barrier oxide reduces diffusion, but the disruption of the surface region produces a heterogeneous region with insulating  $\text{Al}_2\text{O}_3$ , disrupted ceramic, and metallic clusters.

Synchrotron-radiation photoemission experiments used the 3-m toroidal grating monochromator and beam line ( $10 \leq h\nu \leq 130$  eV) at the Wisconsin Synchrotron Radiation Center. Photoelectron energy analysis was done with a double-pass cylindrical mirror analyzer. The photocurrent from a Ni mesh in the monochromatized photon beam was used to monitor the photon flux. The  $\text{YBa}_2\text{Cu}_3\text{O}_{6.9}$  samples were  $\sim 93\%$  dense and polycrystalline with a superconducting transition temperature of  $\sim 92$  K. Clean surfaces were prepared *in situ* by fracturing bulk samples at operating pressures of  $8 \times 10^{-11}$  Torr. Adatoms of Al and In were deposited at  $< 2 \times 10^{-10}$  Torr at a rate of  $\sim 1$  Å/min. Valence-band and core-level energy distribution curves (EDC's) were acquired at each coverage at room temperature.

In Fig. 1 we show representative energy distribution

curves for Al depositions,  $\Theta$ , from 0 to 94 Å. These spectra were taken at a photon energy of 105 eV to use the phenomenon of resonance photoemission to emphasize the Ba-derived emission.<sup>6,16</sup> They have been normalized to the same maximum height for visual clarity. The Ba  $5p_{3/2,1/2}$  and  $5s$  shallow core-level maxima appear at 13.7 and 29.0 eV, and there is a low-bonding-energy shoulder which reflects the Cu  $d^8$  final-state satellite, as discussed by others.<sup>6</sup> Valence-band emission within  $\sim 7.5$  eV of the Fermi level  $E_F$  arises from hybridized Cu  $3d$ -O  $2p$  bands.<sup>11-15</sup> Emission from states near  $E_F$  is very small, consistent with band-structure calculations, and originates from Cu-O antibonding bands which cross  $E_F$ .<sup>14,15</sup> Structure at  $-9.1$  eV has been observed in all previous photoemission studies, but its origin remains unknown. Its intensity scales with the Ba  $5p$  emission and we suspect it is due to a final state Ba- $5p$ -related process.

Valence-band spectra for Al depositions between 0.25 and 14 Å show rapid reduction in emission from states near  $E_F$ , implying the destruction of Cu-O bonds in the surface and near-surface region. (This can be seen better with lower photon energies and expanded energy scales, or when difference curves of the sort shown in Ref. 10 are created.) These states are responsible for superconductivity, and our results indicate that they are very sensitive to the presence of reactive metal adatoms. At the same time, the dominant valence-band features are also modified by the deposition of Al, and there is an asymmetric broadening to higher binding energy. This reflects the formation of Al-O bonds and the lowering in energy of the O  $2p$ -derived levels. Hence, the Al-O bonding occurs at the expense of Cu-O bonds as the Al-O phases nucleate. By 14-Å deposition, these changes are almost stabilized and the dominant O  $2p$ -derived peak appears at 6.5 eV. Our results also show enhanced emission near  $E_F$  after the deposition of 14 Å of Al, and there is a clear Fermi-level edge by 23 Å as a metallic phase grows on the reacted region. It is important to note that the cross section for the Al valence band is small, much less than that of O  $2p$ , and the amount of Al metal on the surface cannot

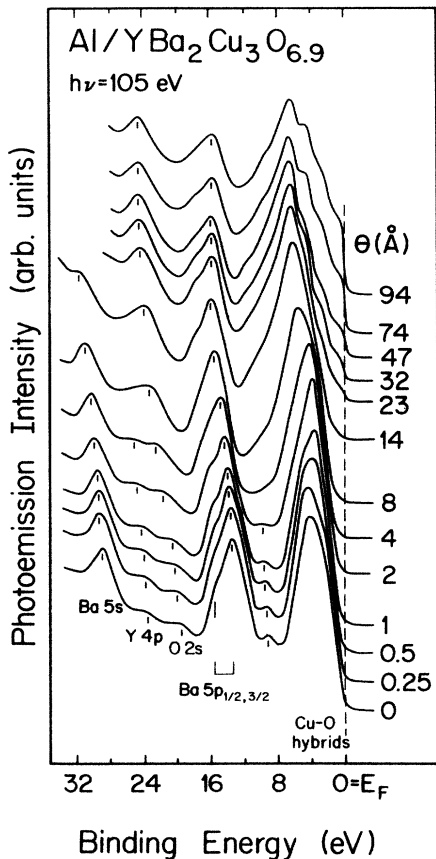


FIG. 1. Valence-band photoemission spectra for Al/YBa<sub>2</sub>Cu<sub>3</sub>O<sub>6.9</sub> taken at  $h\nu=105$  eV to resonantly enhance the Ba-derived features. The deposition of Al induces reaction, the loss of states near  $E_F$ , and chemical shifts as discussed in the text.

be inferred by simple inspection of the heights of different valence-band features.

The results of Fig. 1 show that the O 2*s*-derived feature at 20.5 eV gradually shifts to a final position at 24.4 eV, consistent with the formation of an oxide phase which ultimately becomes fully reacted and stable.<sup>17,18</sup> It is interesting to note that, although the atomic fraction of O in YBa<sub>2</sub>Cu<sub>3</sub>O<sub>6.9</sub> is comparable to that in Al<sub>2</sub>O<sub>3</sub>, the O 2*s* feature for Al<sub>2</sub>O<sub>3</sub> is substantially more prominent. This suggests that the shallow O 2*s* electrons are involved in band formation sufficiently that their photoionization cross section changes (see, for example, the band calculations for Al<sub>2</sub>O<sub>3</sub> in Ref. 17).

The deposition of Al also induces a substantial Ba 5*p* chemical shift of  $\sim 2.3$  eV without obvious spectral change. The Ba 5*s* feature shows the same behavior before it is obscured by strong Al LMM Auger emission. The shift of the Ba features tracks the evolution of the Al<sub>2</sub>O<sub>3</sub> phase, being most pronounced at low coverage but saturating by  $\sim 14$  Å. Moreover, the Ba emission persists as metallic Al grows. It is clear that the chemical environment of Ba in the disrupted region is very different from that in the superconductor. It is also clear that Ba present in the form of the grain-boundary contaminant is also

modified by the deposition of Al.

It is significant that neither the O 2*s* (in Al<sub>2</sub>O<sub>3</sub>) nor the Ba 5*p* features were completely attenuated by the growth of metallic Al. Since 95% of the primary photoelectrons come from a depth of three times the electron mean free path (in normal emission), the deposition of  $\sim 20$  Å would have eliminated all substrate features if the overlayer were homogeneous. Instead, the deposition of  $\sim 70$  Å of Al after metallic Al starts to form fails to cover the reacted region. This implies that Al forms islands or clusters on the Al<sub>2</sub>O<sub>3</sub> layer. These do not cover the surface homogeneously and allow the detection of the substrate-oxide signal. The formation of a continuous metallic overlayer would then be delayed until much higher coverage.

To further demonstrate that Cu–O bonds in the superconductor suffer when Al adatoms interact with the substrate, we show in Fig. 2 EDC's taken at  $h\nu=76$  eV. At this photon energy, the Ba core-level emission is relatively weak but the Cu features are enhanced. Comparison to the clean-surface results of Fig. 1 reveals that the Cu *d*<sup>8</sup> satellite now dominates and that the Ba emission is a weak shoulder. From Fig. 2, we can clearly identify the *d*<sup>8</sup> final-state satellite of the Cu<sup>2+</sup> initial state at 12.4 eV, as observed by others.<sup>6</sup> For studies of interface evolution, this resonantly enhanced satellite can be used to determine changes in the nominal Cu valence. Indeed, the results of Fig. 2 show that the Cu<sup>2+</sup> satellite diminishes rapidly with coverages and disappears at  $\Theta=4$  Å. This demonstrates a redistribution of charge such that nominal Cu<sup>2+</sup> atoms in the superconductor are converted to Cu<sup>1+</sup>. Examination of the results of Ref. 18 shows that the Cu<sup>1+</sup> satellite is substantially weaker than that of Cu<sup>2+</sup> and,

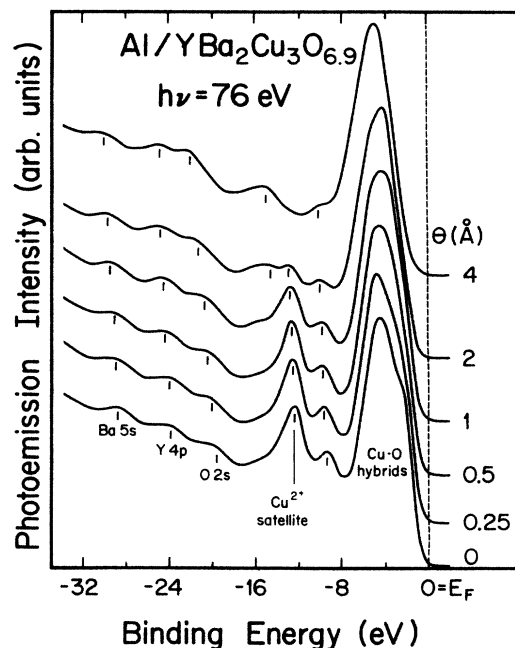


FIG. 2. Valence-band photoemission spectra for Al/YBa<sub>2</sub>Cu<sub>3</sub>O<sub>6.9</sub> which emphasize the Cu<sup>2+</sup> satellite at 12.4 eV, showing that the deposition of Al leads to the rapid loss of the nominal Cu<sup>2+</sup> configuration in the probed region.

moreover, that it overlaps with the Ba 5*p* peak. These results, together with the loss of emission at the Fermi level and the formation of Al<sub>2</sub>O<sub>3</sub>, confirm that reactive adatoms of Al remove O from the superconductor and *all* of the Cu atoms within the probe depth undergo a transition from Cu<sup>2+</sup> to lower valence states.

Additional insight into the development of the Al-based overlayer can be found from the evolving Al 2*p* core-level spectra. As shown in Fig. 3, the deposition of sub-angstrom amounts of Al produces a broad peak which shifts to higher binding energy and increases in intensity with coverage. This shifting is consistent with the O 2*s* results of Figs. 1 and 2 and indicates the progressive formation of a stable aluminum oxide. The Al 2*p* results also show that a second Al feature due to metallic Al is observed at a fixed binding energy before the oxide is fully stabilized. We conclude that reactions on the surface are heterogeneous with metal nucleation at one site while oxidation continues at another due to the details of the vari-

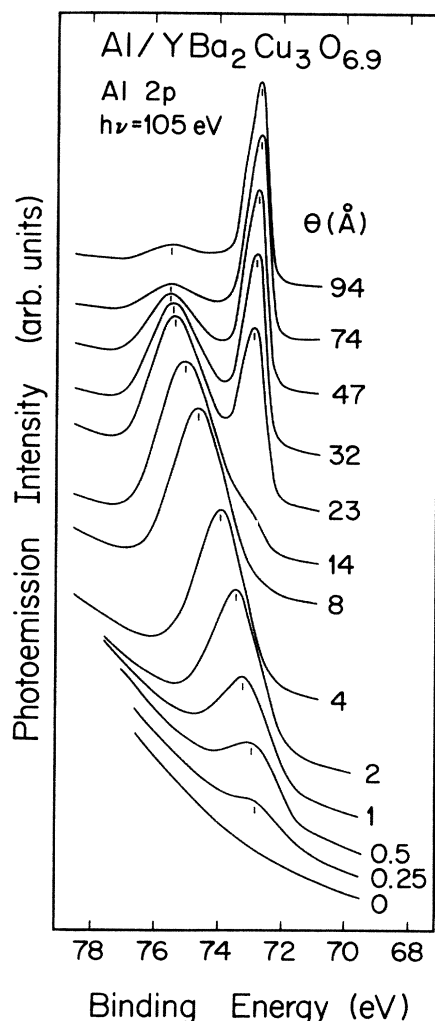


FIG. 3. Al 2*p* core-level spectra for Al/YBa<sub>2</sub>Cu<sub>3</sub>O<sub>6.9</sub>, showing the formation of Al–O bonding configurations which evolve with coverage but stabilize after ~23 Å. The low-energy component indicates the growth of metallic Al clusters.

ous processes. (Heterogeneous growth is also observed for metal-semiconductor interfaces, such as Al/InSb, and is not unique to these ceramics.) The present results indicate that this competition is nearly complete by 23 Å, which corresponds to the coverage at which a metallic Fermi-level cutoff was clearly seen in the valence-band spectra. The width of the oxide peak can be attributed to stoichiometry variations and chemically inequivalent sites. The final Al 2*p* energy separation of oxide and metal of 2.7 eV compares favorably to what has been observed during the oxidation of Al.<sup>18</sup>

Quantitative examination of the integrated Al 2*p* emission shows that the total emission increases with coverage and saturates slowly. At intermediate coverages of 14–23 Å there is competition between oxidation and metal nucleation because of the heterogeneous nature of the surface, as inferred from Figs. 1–3. At higher coverage, there is gradual attenuation of the oxide component. However, the 1/*e* rate at which the oxide emission is reduced is ~40 Å and is inconsistent with layer-by-layer growth of Al (photoelectron mean free path of ~5 Å at kinetic energies of ~23 eV). This supports the assertion that Al metal nucleates on the oxide layer when the oxide inhibits oxygen diffusion from the substrate. The metal nuclei grow with coverage, but are relatively inefficient at covering the substrate. Such clustering is not unexpected for Al deposition onto Al<sub>2</sub>O<sub>3</sub>.

For comparison to the Al 2*p* results, we also determined the Ba 5*p* attenuation curve based on EDC's taken at 105 eV photon energy. The results exhibit rapid attenuation for  $\Theta \leq 4$  Å with a 1/*e* decay rate of ~6 Å which is close to what is expected for electrons of these kinetic energies. Although the complex topology of the starting surface makes quantitative assessments uncertain, this 1/*e* length is consistent with the growth of a passivating oxide along the surface. It further supports the contention that the grain-boundary contaminant phase is not stable in the presence of adatoms of Al. The rate of decay of the Ba emission is then much slower after 14 Å when metallic Al clustering occurs (the 1/*e* rate of ~30 Å is comparable to that for the Al oxide when account is taken of the different photoelectron energies).

Studies analogous to those discussed above were also undertaken for the In/YBa<sub>2</sub>Cu<sub>3</sub>O<sub>6.9</sub> system. The valence-band results (not shown because of space limitations) demonstrate that there is substantial disruption of the Cu–O states at *E<sub>F</sub>*, as is observed for the more reactive metals. Analogous chemical shifts are observed for Ba and O, and the Cu *d*<sup>8</sup> satellite is quenched. Even the behavior for the 9.1 eV feature is similar. At ~8 Å of In deposition, the metallic Fermi-level cutoff appears and we conclude that the reacted layer is thinner than for Al. In 4*d* core-level spectra show a broad, structureless In–O feature at low coverage and the appearance of the well-defined spin-orbit-split doublet characteristic of metallic In for depositions as low as 4 Å. Line-shape analysis shows that the In–O intensity decreases with increasing coverage after metallic In starts to nucleate and the large 1/*e* length of ~50 Å for In–O indicates that the cluster formation again occurs. Although there are differences in detail for Al and In overlayers, our results show parallel

behavior. For both systems, we observe oxygen removal from the substrate and substrate disruption, oxidation of the metal adatoms at low coverage, and nucleation and growth of metallic clusters of Al or In after the passivating layer thickness impedes oxygen transport. Disruption at low coverage is accompanied by the loss of states at  $E_F$  which participate in conduction in these materials. Likewise, the Cu valence at the surface changes from  $\text{Cu}^{2+}$ , and chemically different environments are observed for Ba and Y as O is drawn from the superconductor.

The Minnesota program was supported by the U.S. Office of Naval Research under Grant No. N00014-87-K-0029 and the University of Minnesota. The work at Argonne National Laboratory was supported by the U.S. Department of Energy under Contract No. W-31-109-Eng-38. The synchrotron radiation experiments were done at the Wisconsin Synchrotron Radiation Center (which is supported by the National Science Foundation), and the support of the staff of that laboratory is gratefully acknowledged.

<sup>1</sup>Listings of recent papers regarding high-temperature superconductors appear in *Phys. Rev. Lett.* **58**, No. 20 (1987); **59**, No. 1 (1987); and *Jpn. J. Appl. Phys.* **26**, No. 4 (1987).

<sup>2</sup>P. Steiner, J. Albers, V. Kinsinger, I. Sander, B. Siegart, S. Hüfner, and C. Politis, *Z. Phys. B* **66**, 275 (1987).

<sup>3</sup>B. Reihl, T. Riesterer, J. G. Bednorz, and K. A. Müller, *Phys. Rev. B* **35**, 8804 (1987).

<sup>4</sup>P. D. Johnson, S. L. Qin, L. Liang, M. W. Ruckman, M. Strongin, S. L. Hulbert, R. F. Garrett, B. Sinkovic, N. V. Smith, R. J. Cava, C. S. Jee, D. Nichols, E. Kaczanowicz, R. E. Salomon, and J. E. Crow, *Phys. Rev. B* **35**, 8811 (1987).

<sup>5</sup>A. Fujimori, E. Takayama-Muromachi, Y. Uchida, and B. Okai, *Phys. Rev. B* **35**, 8814 (1987).

<sup>6</sup>R. L. Kurtz, R. L. Stockbauer, D. Mueller, A. Shih, L. E. Toth, M. Osofsky, and S. A. Wolf, *Phys. Rev. B* **35**, 8818 (1987); M. R. Thuler, R. L. Benbow, and Z. Hurych, *ibid.* **26**, 689 (1982).

<sup>7</sup>M. Onellion, Y. Chang, D. W. Nilis, R. Joynt, G. Margaritondo, N. G. Stoffel, and J. M. Tarascon, *Phys. Rev. B* **36**, 819 (1987).

<sup>8</sup>J. A. Yarmoff, D. R. Clarke, W. Drube, V. O. Karlsson, A. Taleb-Ibrahimi, and F. J. Himpsel, *Phys. Rev. B* **36**, 3967 (1987).

<sup>9</sup>Y. Gao, T. J. Wagener, J. H. Weaver, A. J. Arko, B. Flandermeyer, and D. W. Capone II, *Phys. Rev. B* **36**, 3971 (1987); T. J. Wagener, Y. Gao, J. H. Weaver, A. J. Arko, B. Flandermeyer, and D. W. Capone II, *ibid.* **36**, 3899 (1987).

<sup>10</sup>J. H. Weaver, Y. Gao, T. J. Wagener, B. Flandermeyer, and D. W. Capone II, *Phys. Rev. B* **36**, 3975 (1987).

<sup>11</sup>L. F. Mattheiss, *Phys. Rev. Lett.* **58**, 1028 (1987).

<sup>12</sup>Jaejun Yu, A. J. Freeman, and J.-H. Xu, *Phys. Rev. Lett.* **58**, 1035 (1987).

<sup>13</sup>W. Weber, *Phys. Rev. Lett.* **58**, 137 (1987).

<sup>14</sup>W. E. Pickett and H. Krakauer, *Phys. Rev. B* **35**, 7252 (1987).

<sup>15</sup>L. F. Mattheiss and D. R. Hamann, *Solid State Commun.* **63**, 395 (1987).

<sup>16</sup>*Photoemission in Solids*, edited by L. Ley and M. Cardona (Springer-Verlag, New York, 1973).

<sup>17</sup>I. P. Batra and S. Ciraci, *Phys. Rev. Lett.* **39**, 774 (1977); *Phys. Rev. B* **28**, 982 (1983).

<sup>18</sup>W. Eberhardt, *Surf. Sci.* **75**, 709 (1978); W. J. Gignac, R. S. Williams, and S. P. Kowalczyk, *Phys. Rev. B* **32**, 1237 (1985).